

Superradiant phase transitions in the quantum Rabi model: Overcoming the no-go theorem through anisotropy

Tian Ye and Yan-Zhi Wang

Anhui Province Key Laboratory for Control and Applications of Optoelectronic Information Materials,
Department of Physics, Anhui Normal University, Wuhu 241000, China

Xiang-You Chen and Qing-Hu Chen*

Zhejiang Key Laboratory of Micro-Nano Quantum Chips and Quantum Control,
School of Physics, Zhejiang University, Hangzhou 310027, China and
Collaborative Innovation Center of Advanced Microstructures, Nanjing University, Nanjing 210093, China

Hai-Qing Lin†

Institute for Advanced Study in Physics and School of Physics, Zhejiang University, Hangzhou, 310058, China
(Dated: December 12, 2024)

Although the superradiant phase transition (SRPT) is prohibited in the paradigmatic quantum Rabi model due to the no-go theorem caused by the \mathbf{A} -square term, we demonstrate two distinct types of SRPTs emerging from the normal phase in the anisotropic quantum Rabi model. A discontinuous phase transition between the two types of superradiant phases also emerges in the presence of a strong \mathbf{A} -square term. Additionally, a rich phase diagram featuring a triple point, which connects first- and second-order phase transitions, is derived analytically and confirmed through numerical diagonalization at large effective system sizes. Finally, distinct critical behavior at the triple point is revealed and contrasted with that of a single continuous SRPT. This work may open a new avenue for observing SRPTs in their intrinsic form without altering the \mathbf{A} -square term, while also offering a practical platform for exploring rich quantum phenomena.

PACS numbers: 05.30.Rt, 42.50.Ct, 42.50.Pq, 05.70.Jk

I. INTRODUCTION

The Dicke model (DM) describes the interaction between a collection of two-level atoms (qubits) and a single-mode photon field [1], making it a paradigmatic model in quantum optics. In the thermodynamic limit of infinite qubits, the Dicke model (DM) theoretically undergoes a superradiant phase transition (SRPT), characterized by macroscopic excitation of the photon field, at both finite [2, 3] and zero temperatures [4].

Observing an equilibrium SRPT in experiments has long been challenging due to the inability to access sufficiently strong qubit-cavity coupling in cavity quantum electrodynamics (QED). Recent advancements in solid-state quantum platforms and quantum simulations, such as superconducting circuit QED [5–7], trapped ions [8, 9], and cold atoms [10], have enabled light-matter interactions to reach the ultrastong and even deep-strong coupling regimes. It has inspired several theoretical works on the SRPT in the Dicke model [11, 12]. In particular, the few-component SRPT has been explored in the quantum Rabi model (QRM) [13], which is a single-atom version of the DM [14], in the limit of infinite qubit-to-cavity frequency ratio. Since then, the SRPT has been studied in various few-component models, including the Jaynes-

Cummings model [15], the anisotropic QRM [16, 17], and the quantum Rabi triangle [18]. Notably, the SRPTs of the DM and QRM belong to the same universality class, even with anisotropic qubit-cavity coupling.

Despite this renewed possibility, the experimental realization of the SRPT remains debated and an open question to this day [19–32]. In cavity QED, Rzażeskimo *et al.* argued that the \mathbf{A} -square term, originating from the minimal coupling Hamiltonian, would forbid the SRPT of the DM at any finite coupling strength if the Thomas-Reich-Kahn (TRK) sum rule for the atom is properly considered [19]. This no-go theorem also applies to the SRPT of the QRM [13]. Based on the effective model of circuit QED, Nataf and Ciuti proposed that the TRK sum rule in cavity QED could be violated, allowing the SRPT to occur in principle [22]. Viehmann *et al.* questioned whether, even with a complete microscopic treatment, the no-go theorem of cavity QED still applies to circuit QED [23]. These arguments focus on whether the TRK sum rule differs in various systems [23, 24], raising a significant controversy over whether the \mathbf{A} -square term can be engineered in the superconducting qubit circuit platform [25–28]. On the other hand, the validity of the two-level approximation, a crucial step in constructing the DM in various solid-state devices, as well as the applicability of Coulomb and electric dipole gauges and different experimental schemes leading to the varying \mathbf{A} -square term, are widely discussed in the literature (see [33–35], and the references therein). Consensus has yet to be reached, and the no-go theorem remains the most

*Electronic address: qhchen@zju.edu.cn

†Electronic address: hqlin@zju.edu.cn

controversial subject.

To overcome the no-go theorem and realize the SRPT, several groups have introduced additional extrinsic factors that extend beyond the original DM and QRM. It was suggested that the no-go theorem does not apply to the three-level DM, making the SRPT possible [36]. By adding an interaction between atoms in the DM, Liu *et al.* found that an SRPT can occur in a specific parameter regime [37]. Jaako *et al.* proposed that a circuit QED system with a symmetrically coupled single resonator can contain interactions between qubits, enabling the achievement of an SRPT in the two-qubit QRM [26]. Considering the hopping between cavity bosons at two sites, the competition between the \mathbf{A} -square term and the boson hopping term can lead to the appearance of the SRPT in the two-site QRM [38]. Recently, Chen *et al.* introduced an antisqueezing effect into the NMR quantum simulator, directly alleviating the constraint of the no-go theorem and realizing the SRPT in the QRM with the \mathbf{A} -square term [39].

It would be interesting to go beyond the no-go theorem intrinsically by manipulating the internal factors of the original DM and QRM without altering the \mathbf{A} -square term subject to the TRK sum rule. In this paper, we investigate the anisotropic QRM with varying coupling strengths of the rotating and counterrotating wave terms and arbitrary \mathbf{A} -square terms. It is well known that the anisotropic QRM without the \mathbf{A} -square term can exhibit an SRPT [16, 17]. Recently, multiple ground-state instabilities have been observed in the anisotropic QRM [40], driven solely by the anisotropy. A natural question arises: can the SRPT be induced by anisotropy in the anisotropic QRM with the \mathbf{A} -square term? Interestingly, we find not only two types of SRPT, but also first-order phase transitions between them, and further construct a rich phase diagram that includes a triple point.

The paper is organized as follows: In Sec. II, we briefly introduce the anisotropic quantum Rabi model with the \mathbf{A} -square term. In Sec. III, using the Bogoliubov transformation, we derive a renormalized anisotropic QRM without the \mathbf{A} -square term. We then analytically obtain two types of SRPT and a rich phase diagram in the large limit of the frequency ratio. These analytical findings are confirmed numerically in Sec. IV, where the distinguishing critical behavior at the triple point is also detected through finite-size scaling analysis. Finally, conclusions are drawn in Sec. V. The Appendix analytically presents the energy-gap critical exponents at both the triple point and the standard SRPT based on an effective Hamiltonian.

II. THE ANISOTROPIC QRM WITH THE \mathbf{A} -SQUARE TERM

The anisotropic QRM with the \mathbf{A} -square term can be described as follows.

$$H = \omega a^\dagger a + \frac{\Delta}{2} \sigma_z + g [(a\sigma_+ + a^\dagger\sigma_-) + \tau(a\sigma_- + a^\dagger\sigma_+)] + D(a + a^\dagger)^2, \quad (1)$$

where the operator a (a^\dagger) creates (annihilates) a photon of the electromagnetic mode with frequency ω , while Δ represents the qubit energy splitting. The operators $\sigma_\pm = \frac{1}{2}(\sigma_x \pm i\sigma_y)$ excite (relax) the qubit from $|+\rangle$ ($|-\rangle$) to $|-\rangle$ ($|+\rangle$), where $|\pm\rangle$ denotes the excited (ground) state of the qubit. Here, σ_i ($i = x, y, z$) represents the Pauli matrices. The coupling strength is denoted by g , τ is the anisotropic parameter of the coupling (which can take both positive and negative values for various applications), and D is the strength of the \mathbf{A} -square term.

The anisotropic QRM bridges the gap between the QRM and the Jaynes-Cummings model. Specifically, as the anisotropic parameter varies from $\tau = 1$ to $\tau = 0$, the model transitions continuously from the QRM to the Jaynes-Cummings model. Notably, the anisotropic QRM retains the same \mathbb{Z}_2 symmetry as the QRM, with the parity operator $P = -\sigma_z e^{i\pi a^\dagger a}$, even when the \mathbf{A} -square term is included.

To relate to the no-go theorem for the SRPT in the QRM, we define the strength of the \mathbf{A} -square term as $D = \kappa D_0$, where κ is a nonnegative constant and $D_0 = \frac{g^2}{\Delta}$. When $\kappa = 1$, it represents the minimum strength of the \mathbf{A} -square term, as dictated by the TRK sum rule for the atom. In the original light-matter interaction platform, where a real atom is coupled to the photonic mode, the \mathbf{A} -square term arises from $(\mathbf{p} - q\mathbf{A})^2/2m$ in the minimal coupling Hamiltonian, where \mathbf{p} and \mathbf{A} represent the electron momentum operator and the electromagnetic vector potential, respectively. Theoretically, this \mathbf{A} -square term is often neglected in the literature, even in the strong coupling regime, which leads to the SRPT being present and extensively studied for $\kappa = 0$. Since the \mathbf{A} -square term may be non-negligible in both cavity and circuit QEDs in various ways, its strength can be adjusted to arbitrary values for broader applications.

Due to the ongoing progress in quantum technology, the anisotropic QRM can now be realized using various schemes, such as superconducting qubit circuits [11, 41, 42], electron gases with both Rashba and Dresselhaus spin-orbit interactions [43], and spin qubits coupled to anisotropic ferromagnets [44]. Specifically, in circuit QED, a large SQUID generates an electromagnetic field and is inductively coupled to a qubit realized by another SQUID. By including both the circuit inductance and the mutual inductance between the two SQUIDs, the anisotropic qubit-photon coupling can be simulated, provided that the capacitive interaction between these two SQUIDs is engineered to be negligible. Another realization of the anisotropic QRM has been proposed using an

ensemble of NV center spins in diamond, coupled to the quantized magnetic field of a superconducting microwave cavity [45]. A driving field induces coupling between two excited states of an artificial atom through two-photon Raman transitions within the cavity. The two possible transitions between the atomic states involve either the absorption or emission of a cavity photon. This results in both rotating-wave terms ($a^\dagger\sigma_-$ and $a\sigma_+$) and counter-rotating-wave terms ($a^\dagger\sigma_+$ and $a\sigma_-$), thereby yielding the anisotropic QRM. In these experiments, the effect of the \mathbf{A} -square term is worth considering.

III. RECOVERY OF THE SUPERRADIANT PHASE TRANSITION THROUGH ANISOTROPY

A. Bogoliubov transformed Hamiltonian

To facilitate the analytical study, we first eliminate the \mathbf{A} -square term by introducing new bosonic operators, derived from the Bogoliubov transformation applied to the original operators.

$$b = \mu a + \nu a^\dagger, \quad (2a)$$

$$b^\dagger = \mu a^\dagger + \nu a. \quad (2b)$$

To ensure the bosonic nature of the new operators, the coefficients must satisfy the constraint $\mu^2 - \nu^2 = 1$. If the condition $D(\mu - \nu)^2 - \omega\mu\nu = 0$ is satisfied, the original Hamiltonian can be transformed into a form without the \mathbf{A} -square term,

$$H = \omega' b^\dagger b + \frac{\Delta}{2} \sigma_z + g' [(b\sigma_+ + b^\dagger\sigma_-) + \tau'(b\sigma_- + b^\dagger\sigma_+)], \quad (3)$$

where $\omega' = (\mu + \nu)^2\omega$, $g' = g(\mu - \tau\nu)$, and $\tau' = (\tau\mu - \nu)/(\mu - \tau\nu)$. For later reference, we outline two constraint conditions for μ and ν ,

$$\gamma = (\mu + \nu)^2 = \sqrt{1 + \kappa\tilde{g}^2}, \quad (4)$$

$$\zeta = \frac{\nu}{\mu} = 1 + \frac{2}{\kappa\tilde{g}^2} - \sqrt{\left(1 + \frac{2}{\kappa\tilde{g}^2}\right)^2 - 1}. \quad (5)$$

Here, the rescaled coupling strength is given by $\tilde{g} = 2g/\sqrt{\omega\Delta}$. It is important to note that the new transformed parameters, g' and τ' , can extend into the negative regime, even when the original parameters $g > 0$ and $\tau > 0$. This extension may lead to a richer phase diagram than that of the standard anisotropic QRM.

B. Superradiant phase transitions enriched by anisotropy

In the standard QRM, the effective system size is defined by the frequency ratio $\eta = \Delta/\omega$. The quantum phase transition (QPT) occurs in the thermodynamic

limit, i.e., as $\eta \rightarrow \infty$, while the rescaled coupling strength \tilde{g} remains finite. To investigate the superradiant phase transition (SRPT) in the current anisotropic model with the \mathbf{A} -square term, we similarly define $\eta' = \Delta/\omega' \rightarrow \infty$ and keep the auxiliary coupling $\tilde{g}' = 2g'/\sqrt{(\omega'\Delta)}$ finite.

In terms of the field quadratures, $x = (b + b^\dagger)/\sqrt{2}$ and $p = i((b^\dagger - b)/\sqrt{2})$, we rewrite the Hamiltonian (3) in the following rescaled form:

$$\begin{aligned} \tilde{H} &= \frac{H}{\Delta} = \frac{x^2 + p^2}{2\eta'} + \frac{1}{2}\sigma_z \\ &+ \frac{\tilde{g}'}{\sqrt{8\eta'}} [(1 + \tau')x\sigma_x - (1 - \tau')p\sigma_y]. \end{aligned} \quad (6)$$

In the thermodynamic limit, the coupling term becomes the leading-order perturbation, proportional to $1/\sqrt{\eta'}$. In particular, this term is off-diagonal in the basis of the eigenvectors of σ_z . To diagonalize this perturbation, we perform the unitary transformation $H_{\text{eff}} = e^{-S}\tilde{H}e^S$, where the $S = -i\tilde{g}'[(1 + \tau')x\sigma_y + (1 - \tau')p\sigma_x]/\sqrt{8\eta'}$. This yields:

$$H_{\text{eff}} \simeq \frac{\gamma(x^2 + p^2)}{2\eta} + \frac{1}{2}\sigma_z + \frac{\gamma\tilde{g}^2}{8\eta} [\xi_x^2 x^2 + (1 - \tau)^2 p^2] \sigma_z,$$

where the coefficient is given by $\xi_x = (1 + \tau)(1 - \zeta)/(1 + \zeta)$.

Focusing on the low-energy states, we project the Hamiltonian onto the spin-down subspace, yielding the effective low-energy Hamiltonian,

$$H_{\text{eff}} \simeq \frac{\gamma}{8\eta} \left\{ 4(x^2 + p^2) - \tilde{g}^2 [\xi_x^2 x^2 + (1 - \tau)^2 p^2] \right\}. \quad (7)$$

Obviously, the first term dominates at weak coupling, indicating the system behaves as a normal oscillator. In the ground state, this corresponds to the normal phase, characterized by the vacuum photonic state. On the other hand, if \tilde{g} becomes large enough, the effective Hamiltonian will become unbounded due to the dominant negative coupling term. Specifically, this leads to the emergence of x -type (p -type) superradiant phase (SRP), signaled by the divergent value of $\langle x^2 \rangle$ ($\langle p^2 \rangle$) in the ground state, similar to what was observed in the original anisotropic QRM [16]

Equating the coefficients of x^2 and p^2 in the effective Hamiltonian (7) gives,

$$\kappa_c = 4\tau / [(1 - \tau)^2 \tilde{g}^2]. \quad (8)$$

The p^2 -type (x^2 -type) term dominates when $\kappa > \kappa_c$ ($\kappa < \kappa_c$) from the perspective of macroscopic photon mode excitation. When $\kappa > \kappa_c$, the vanishing coefficient of the p^2 -type term in the effective Hamiltonian (7) determines the critical coupling point that separates the p -type SRP from the normal phase,

$$\tilde{g}_c^p = \frac{2}{|1 - \tau|} \quad (9)$$

at $\tau \neq 1$ and $\tau < \kappa$ obtained by $\kappa > \kappa_c(\tau, \tilde{g}_c^p)$. Similarly, if $\kappa < \kappa_c$, the vanishing coefficient of the x^2 -type term

yields the critical coupling strength that separates the x-type SRP from the normal phase.

$$\tilde{g}_c^x = \frac{2}{\sqrt{(1+\tau)^2 - 4\kappa}}, \quad (10)$$

at $\tau > \kappa$ obtained by $\kappa < \kappa_c(\tau, \tilde{g}_c^x)$.

Eqs. (9) and (10) describe the critical coupling of the anisotropic QRM without the \mathbf{A} -square term ($\kappa = 0$) [16, 17]. These equations are also consistent with the no-go theorem, which states that for $\kappa \geq 1$ and $\tau = 1$, \tilde{g}_c^p tends to infinity, and a real solution for \tilde{g}_c^x is only possible when $\kappa < 1$ and $\tau = 1$.

Note that \tilde{g}_c^p and \tilde{g}_c^x are subject to $\kappa > \kappa_c$ and $\kappa < \kappa_c$, respectively. From Eq. (8), κ_c depends on the rescaled coupling strength \tilde{g} . For a given κ , when the coupling constant varies and crosses a critical value $\tilde{g}_c^1 = 2\sqrt{\tau/\kappa}/|1-\tau|$ corresponding to $\kappa = \kappa_c$, the macroscopic-excited photon field for x^2 type to p^2 type are interchanged. This implies a first-order phase transition from the x-type SRP to the p-type SRP at the coupling \tilde{g}_c^1 , with $\tau > \kappa$. Interestingly, $\tilde{g}_c^p = \tilde{g}_c^x$ would give a triple critical point at $\tau = \kappa > 1$,

$$\tilde{g}_c^{tri} = \frac{2}{\tau - 1}. \quad (11)$$

A triple critical point does not exist in the anisotropic QRM without the \mathbf{A} -square term. The main analytical results are shown in Fig. 1. Using Eqs. (9) and (10), we plot the boundary of the x^2 -type (or p^2 -type) phase for three typical values of the \mathbf{A} -square strength: (a) $\kappa = 0$, (b) $\kappa = 1$, and (c) $\kappa = 3$. The red solid curves $\tilde{g} = 2\sqrt{\tau/\kappa}/|1-\tau|$ corresponding to $\kappa = \kappa_c$ from Eq. (8) are also plotted in (b) and (c).

As shown in Fig.1(a) for $\kappa = 0$, Eqs.(9) and (10) recover the x -type and p -type SRPs of the anisotropic QRM without the \mathbf{A} -square term [16]. The phase diagram is symmetric, with x -type and p -type SRPs emerging for positive and negative τ , respectively. One type of SRP transitions to the other as τ approaches zero [16].

This symmetric structure is broken in the presence of the \mathbf{A} -square term, as shown in (b) and (c). In the positive- τ regime, the x-type SRP shrinks and is gradually replaced by the p-type SRP as the \mathbf{A} -square term increases. For any finite $\kappa > 0$, Eq. (9) shows that the p-type SRPT of the anisotropic QRM with the \mathbf{A} -square term can always be realized. In the case of $\tau > 0$, as long as $\tau > \kappa$, the x-type SRPT can also be realized. *In other words, for any \mathbf{A} -square strength κ , the SRPT can be driven by anisotropy as long as $\tau \neq 1$, thus overcoming the no-go theorem.*

The analytical results above highlight a remarkable feature of the SRPT induced by anisotropy. The p-type SRPT described by Eq. (9) is independent of the \mathbf{A} -square term as long as $\tau < \kappa$. The effective Hamiltonian (7) explicitly demonstrates the robustness of the p-type SRPT. Note that the relative strength of two p^2 -type terms is unaffected by the \mathbf{A} -square term, indicat-

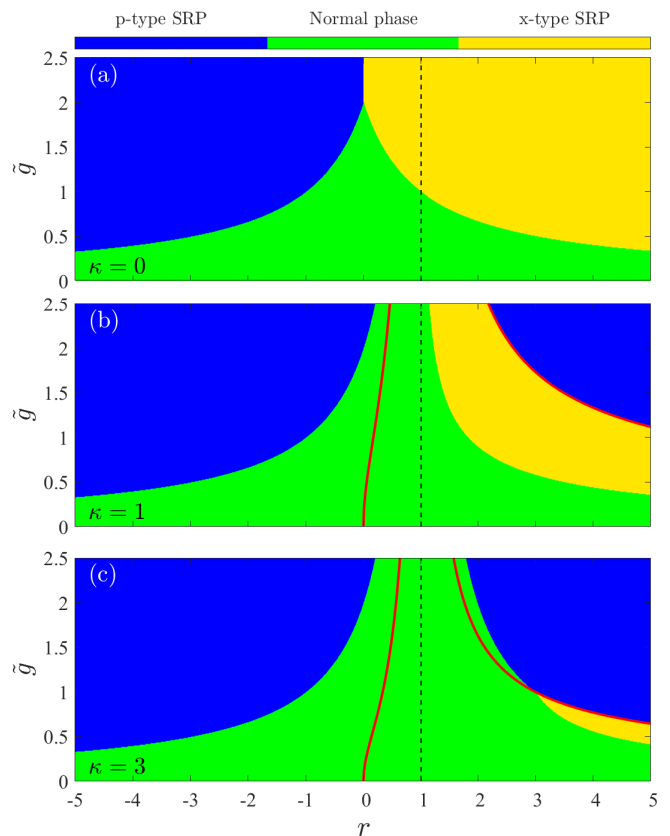


FIG. 1: Phase diagrams of the anisotropic QRM with three typical \mathbf{A} -square terms: (a) $\kappa = 0$, (b) $\kappa = 1$ (minimum value constrained by the TRK sum rule), and (c) $\kappa = 3$. The p- and x-type SRPs are indicated in blue and yellow, respectively, while the normal phase is shown in green. Red solid lines represent $\kappa = \kappa_c$, as given by Eq. (8).

ing that the effective Hamiltonian (7) must become unbounded if $\tilde{g} > \frac{2}{|1-\tau|}$. Furthermore, this unbounded effective Hamiltonian implies macroscopic excitation of the photon mode and the eventual emergence of the SRP. Thus, combined with Eq. (10), it is clear that the x-type SRPT is suppressed as the \mathbf{A} -square term increases, while the p-type SRPT remains robust even with arbitrarily strong \mathbf{A} -square terms. At $\tau = 1$, the p-type SRPT is forbidden regardless of the \mathbf{A} -square term, due to the vanishing p^2 -type coupling ($\propto (1-\tau)^2$) in Hamiltonian (7).

Recently, the superradiant phase transition in the Dicke-Stark model with \mathbf{A} -square terms was studied at both zero and finite temperatures [46]. Using the Holstein-Primakoff transformation of the angular momentum operator, the critical coupling strength for the SRT is derived. The analytical derivation reveals, somewhat ambiguously, that the phase transition occurs for the anisotropy constant $\tau > 1$, even in the absence of the Stark coupling terms. In this work, we find that the SRT can occur in both the $\tau > 1$ and $\tau < 1$ regions, revealing a much richer phase diagram in the context of the QRM.

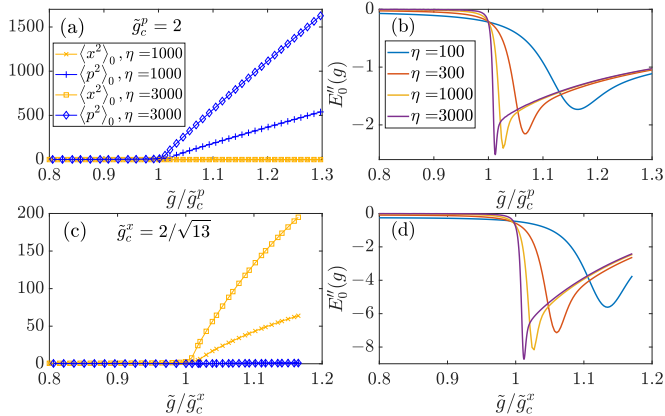


FIG. 2: Characterization of two types of SRPTs at large effective size η : (upper panel) p-type for $\tau = 2, \kappa = 3$ and (lower panel) x-type for $\tau = 4, \kappa = 3$. The position-quadrature square $\langle x^2 \rangle_0$ and the momentum-quadrature square $\langle p^2 \rangle_0$ of the field in the ground state (left panel). The second-order derivatives of the ground-state energy (right panel).

IV. NUMERICAL VERIFICATION AND FINITE-FREQUENCY SCALING ANALYSIS

To validate the analytical findings, numerical diagonalization is performed on the anisotropic QRM with the \mathbf{A} -square term at a large effective sizes η . Typical parameters are $\tau = 2$ and $\tau = 4$ with $\kappa = 3$, corresponding to a p-type SRPT at $\tilde{g}_c^p = 2$ and an x-type SRPT at $\tilde{g}_c^x = 2/\sqrt{13}$, as shown in Fig. 1 (c). Numerical results for the excitation behavior of the ground-state photonic mode (left panel) and the second-order derivatives of the ground-state energy $E''_0(g)$ (right panel) are presented in Fig. 2 for various values of η . It is evident that the system remains unexcited in the normal phase prior to reaching the critical coupling. After the critical coupling of x-type (p-type) SRPT, the position-quadrature square $\langle x^2 \rangle_0 = \langle \psi_0 | x^2 | \psi_0 \rangle$ (momentum-quadrature square $\langle p^2 \rangle_0 = \langle \psi_0 | p^2 | \psi_0 \rangle$) of the field is excited significantly with increasing η , while the other one $\langle p^2 \rangle_0$ ($\langle x^2 \rangle_0$) remains unexcited. This behavior clearly indicates the emergence of x-type (p-type) SRPT. Further evidence is provided by the sudden drop in $E''_0(g)$ around the critical point. Thus, the second-order nature of both x-type and p-type SRPTs is convincingly observed numerically, confirming the analytical findings that anisotropy can overcome the no-go theorem.

We numerically investigate the first-order phase transition from x-type SRP to p-type SRP at the red solid lines corresponding to $\kappa = \kappa_c$ in Fig. 1 (b) and (c). The field-excitation behaviors and the first-order derivative of the ground-state energy $E'_0(g)$ for $\tau = 3, \kappa = 1$ and $\tau = 4, \kappa = 3$ are shown in Fig. 3, where the corresponding transition coupling constants are $\tilde{g}_c^1 = \sqrt{3}$ and $\tilde{g}_c^1 = 4\sqrt{3}/9$, respectively. Before the phase transition, $\langle x^2 \rangle_0$ is significantly excited, while $\langle p^2 \rangle_0$ remains unexcited, indicating the x-type SRP of the system. Across

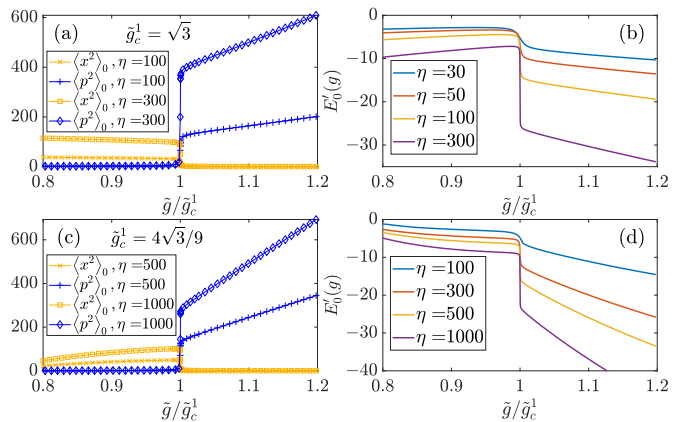


FIG. 3: Characterization of the first-order phase transition from x-type SRP to p-type SRP through large effective size η calculations. (Upper panel) $\tau = 3, \kappa = 1$ and (Lower panel) $\tau = 4, \kappa = 3$. The position-quadrature square $\langle x^2 \rangle_0$ and the momentum-quadrature square $\langle p^2 \rangle_0$ of the field in the ground state (left panel). The first-order derivatives of the ground-state energy (right panel).

the phase transition, the excited field-quadrature square of the photon mode shifts from $\langle x^2 \rangle_0$ to $\langle p^2 \rangle_0$. This indicates a clear transition from x-type SRP to p-type SRP. Additionally, the first-order derivative of the ground-state energy $E'_0(g)$ drops abruptly at the transition point, showing a clear discontinuous trend with increasing η . Therefore, we confirm the first-order nature of the phase transition from x-type SRP to p-type SRP.

In particular, the joint point shown in Fig. 1(c) with $\tau = 3, \tilde{g} = 1$ is of interest, where the phase transition to p-type SRP changes from second order to first order as τ increases. Points such as those determined in Eq. (11) are surrounded by all three types of quantum phases and are therefore termed the triple point. The triple point may provide distinguishing critical properties compared to the original SRPT. To this end, we will extract the critical behaviors of both the standard SRPT and the triple point using finite-size scaling analysis in the following.

In the critical regime of a continuous phase transition, the finite-size scaling function of a physical observable O should take the following form:

$$O(\eta, \tilde{g}) = |1 - \tilde{g}/\tilde{g}_c|^{\beta_O} f(|1 - \tilde{g}/\tilde{g}_c| \eta^\nu),$$

where the frequency ratio η is the effective size of the system, β_O is the critical exponent of the observable O , and ν is the correlation-length critical exponent, which is independent of the observable. Here, we investigate the finite-size scaling behaviors for the order parameter $n_0 = \langle \psi_0 | a^\dagger a | \psi_0 \rangle / \eta$ and energy gap $\epsilon = E_1 - E_0$. The numerical results for the ordinary SRPT at $\tau = 2, \kappa = 3$ are shown in Fig. 4 (a) and (b). Note that the curves for different effective sizes η collapse well onto a single curve, with the observable-independent correlation length exponent $\nu = \frac{2}{3}$ and the critical exponents $\beta_{n_0} = 1$ ($\beta_\epsilon = \frac{1}{2}$) for the order parameter n_0 and energy gap ϵ . It is not

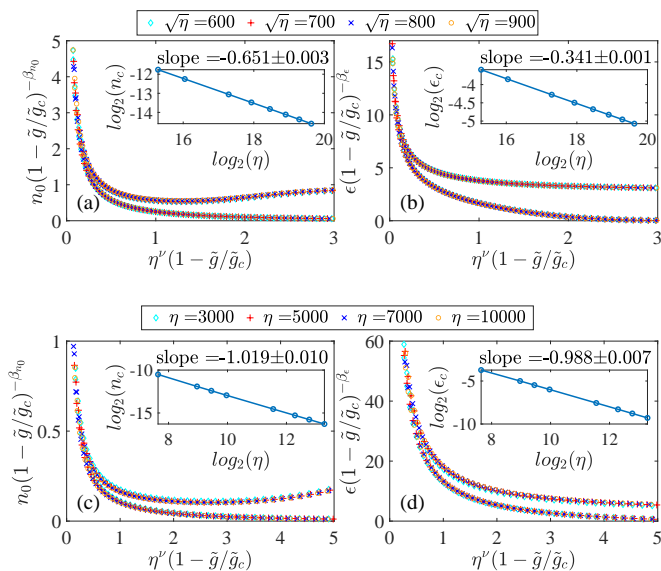


FIG. 4: The finite-size scaling of the order parameter $n_0 = \langle \psi_0 | a^\dagger a | \psi_0 \rangle / \eta$ (left panel) and the energy gap $\epsilon = E_1 - E_0$ (right panel) for the original SRPT with $\tau = 2, \kappa = 3$ (upper panel) and the triple point with $\tau = 3, \kappa = 3$ (lower panel). The size (η) dependence of the order parameter n_c (left panel) and the energy gap ϵ_c (right panel) at the corresponding critical point is shown in the inset, presented in a log-log scale.

surprising that these critical exponents are the same as those of the DM and the QRM [4, 13, 16, 47, 48].

The numerical results for the triple point at $\tau = 3, \kappa = 3$ are shown in Fig. 4 (c) and (d). While the critical exponent of the order parameter β_{n_0} remains unchanged, the correlation-length (energy-gap) critical exponent changes to $\nu^T = 1$ ($\beta_\epsilon^T = 1$), which differs from those in the ordinary SRPT. Nice power-law behavior of the order parameter and the energy gap at critical point ($O_c \propto \eta^{-\gamma_O}$) is also demonstrated in the insets. The fitting value of the scaling exponent γ_O satisfies the scaling law $\gamma_O = \beta_O \nu$ very well, and further confirms the different correlation-length critical exponent at the multi-critical point. Therefore, it can be concluded that the criticality at the triple point differs from that of the ordinary SRPT.

Interestingly, the energy gap exponent at the triple point and in the ordinary SRPT can also be derived analytically using an alternative effective Hamiltonian, as provided in the Appendix.

V. CONCLUSION

In this paper, we investigate the SRPT in the anisotropic QRM with an arbitrary \mathbf{A} -square term. By performing the Bogoliubov and unitary transformations, we derived a low-energy effective Hamiltonian that allows for SRPTs of both x- and p-types, as well as a triple point connecting the first- and second-order QPTs. The

second-order SRPT remains robust even when the \mathbf{A} -square term exceeds the value given by the TRK sum rule, as long as the anisotropic qubit-cavity coupling is present, thus surpassing the limitations of the celebrated no-go theorem. In particular, it is revealed that the x-type superradiant phase is suppressed as the \mathbf{A} -square term increases, whereas the p-type superradiant phase remains robust even for arbitrarily strong \mathbf{A} -square terms. A rich phase diagram for the anisotropic QRM is derived analytically and confirmed by careful numerical diagonalization at large effective sizes. Numerical finite-size scaling analysis reveals that the critical correlation-length exponent and energy-gap exponent $\nu = 1, \beta_\epsilon = 1$ at the triple point differ from $\nu = 2/3, \beta_\epsilon = 1/2$ in the original SRPT. The same energy-gap exponents can also be derived analytically.

In summary, we theoretically propose SRPTs in the anisotropic QRM under a strong \mathbf{A} -square term, as dictated by the TRK sum rule. In this model, aside from anisotropy, no other factors—such as qubit-qubit interactions, suppression of the \mathbf{A} -square terms, inter-cavity hopping, periodic driving, or controlled dissipation—are involved. If the proposed model—anisotropic qubit-cavity coupling systems—is experimentally realized in the deep-strong coupling regime, SRPT may be observed. To date, the equilibrium SRPT has not been convincingly observed in experiments, to the best of our knowledge. This proposal is one of the most practical candidates for the potential observation of SRPT and may also provide a new platform for studying quantum critical phenomena.

ACKNOWLEDGEMENTS This work is supported by the National Natural Science Foundation of China (Grants No. 11834005, 12105001, and 12305009), the National Key R&D Program of China (Grant No. 2022YFA1402701), and the Natural Science Foundation of Anhui Province (Grant No. 2108085QA24).

Appendix: Analytical derivation of the energy-gap critical exponent using an alternative effective Hamiltonian

In this Appendix, we derive an alternative effective Hamiltonian for superradiant phases. Although it is more complicated than Eq. (8) in the main text, it further provides the energy gap and its critical exponent analytically.

To achieve this, we apply the following transformations to the Hamiltonian (6) in the main text: $H^{\text{SR}} = U_{\sigma_y}^\dagger U_{\sigma_z}^\dagger U_n^\dagger \tilde{H}(x+x_0, p+p_0) U_n U_{\sigma_z} U_{\sigma_y}$ where $\tilde{H}(x+x_0, p+p_0)$ denotes the displacing transformation on $\tilde{H}(x, p)$, $U_n = e^{-i(x^2+p^2)\theta_1/2}$, $U_{\sigma_z} = e^{-i\sigma_z\theta_2/2}$ and $U_{\sigma_y} =$

$e^{-i\sigma_y\theta_3/2}$. Thus, H^{SR} is collected as

$$\begin{aligned}
H^{\text{SR}} &= \frac{x^2 + p^2}{2\eta'} \\
&+ \sigma_z [\cos\theta_3 + 2(G^+x_0 \cos\theta_2 - G^-p_0 \sin\theta_2) \sin\theta_3] / 2 \\
&+ x\sigma_x \cos\theta_3 (G_R \cos\theta_- + G_{cR} \cos\theta_+) \\
&- p\sigma_y (G_R \cos\theta_- - G_{cR} \cos\theta_+) \\
&+ C_{\sigma_x}\sigma_x + C_{\sigma_y}\sigma_y + C_{x\sigma_y}x\sigma_y + C_{p\sigma_x}p\sigma_x \\
&+ \frac{x}{\eta'} C_x |\downarrow\rangle \langle\downarrow| + \frac{x}{\eta'} |\uparrow\rangle \langle\uparrow| \{ (x_0 \cos\theta_1 - p_0 \sin\theta_1) \\
&\quad + \eta' \sin\theta_3 (G_R \cos\theta_- + G_{cR} \cos\theta_+) \} \\
&+ \frac{p}{\eta'} C_y |\downarrow\rangle \langle\downarrow| + \frac{p}{\eta'} |\uparrow\rangle \langle\uparrow| \{ (x_0 \sin\theta_1 + p_0 \cos\theta_1) \\
&\quad + \eta' \sin\theta_3 (G_R \sin\theta_- + G_{cR} \sin\theta_+) \}
\end{aligned} \tag{12}$$

where $|\uparrow\rangle(|\downarrow\rangle)$ is the eigenstate of new Pauli matrix σ_z satisfying $\sigma_z |\uparrow\rangle = |\uparrow\rangle$ ($\sigma_z |\downarrow\rangle = -|\downarrow\rangle$), $\theta_{\pm} = \theta_1 \pm \theta_2$, $G_R = \frac{\tilde{g}'}{\sqrt{8\eta'}}$, $G_{cR} = \frac{\tilde{g}'\tau'}{\sqrt{8\eta'}}$, $G^+ = G_R + G_{cR}$, $G^- = G_R - G_{cR}$, and the coefficients $C_{\sigma_x}, C_{\sigma_y}, C_{x\sigma_y}, C_{p\sigma_x}, C_x, C_y$ are list below

$$\begin{aligned}
C_{\sigma_x} &= -\sin\theta_3/2 + (G^+x_0 \cos\theta_2 - G^-p_0 \sin\theta_2) \cos\theta_3; \\
C_{\sigma_y} &= -(G^+x_0 \sin\theta_2 + G^-p_0 \cos\theta_2); \\
C_{x\sigma_y} &= G_R \sin\theta_- - G_{cR} \sin\theta_+; \\
C_{p\sigma_x} &= \cos\theta_3 (G_R \sin\theta_- + G_{cR} \sin\theta_+); \\
C_x &= (x_0 \cos\theta_1 - p_0 \sin\theta_1) \\
&\quad - \eta' \sin\theta_3 (G_R \cos\theta_- + G_{cR} \cos\theta_+); \\
C_y &= (x_0 \sin\theta_1 + p_0 \cos\theta_1) \\
&\quad - \eta' \sin\theta_3 (G_R \sin\theta_- + G_{cR} \sin\theta_+).
\end{aligned}$$

It should be noted that if the transformation coefficients satisfy $C_{\sigma_x} = C_{\sigma_y} = C_{x\sigma_y} = C_{p\sigma_x} = 0$, the fifth line of Eq. (12) is eliminated. Moreover, if C_x and C_p vanish, the influence of the last four lines on the ground state can be neglected in the thermodynamic limit. Therefore, when these conditions are satisfied, Hamiltonian (12) reduces to the same form as Hamiltonian (6) before the transformations,

$$\begin{aligned}
\tilde{H}^{\text{SR}} &= H^{\text{SR}} \cos\theta_3 = \frac{x^2 + p^2}{2\eta''} + \frac{1}{2}\sigma_z \\
&+ \frac{\tilde{g}''}{\sqrt{8\eta''}} [(1 + \tau'')x\sigma_x - (1 - \tau'')p\sigma_y], \tag{13}
\end{aligned}$$

where the new coefficients are

$$\begin{aligned}
\eta'' &= \frac{\eta'}{\cos\theta_3} \\
\tilde{g}'' &= \frac{\tilde{g}'\sqrt{\cos\theta_3}}{2} \{ \cos\theta_- (\cos\theta_3 + 1) \\
&\quad + \tau' \cos\theta_+ (\cos\theta_3 - 1) \}, \\
\tau'' &= \frac{\cos\theta_- (\cos\theta_3 - 1) + \tau' \cos\theta_+ (\cos\theta_3 + 1)}{\cos\theta_- (\cos\theta_3 + 1) + \tau' \cos\theta_+ (\cos\theta_3 - 1)}.
\end{aligned}$$

Next, performing a similar unitary transformation $H_{\text{eff}}^{\text{SR}} = e^{-S} \tilde{H}^{\text{SR}} e^S$ with the generator $S = -i\tilde{g}'' [(1 + \tau'')x\sigma_y + (1 - \tau'')p\sigma_x] / \sqrt{8\eta''}$, the effective low-energy Hamiltonian for the SRP is obtained as

$$H_{\text{eff}}^{\text{SR}} \simeq \frac{(x^2 + p^2)}{2\eta''} - \frac{\tilde{g}''^2}{8\eta''} [(1 + \tau'')^2 x^2 + (1 - \tau'')^2 p^2]. \tag{14}$$

The energy gap thus is

$$\epsilon = \frac{\gamma\omega}{4} \sqrt{(4 - C_\epsilon^x \cos^3\theta_3)(4 - C_\epsilon^p \cos\theta_3)}$$

with the coefficients $C_\epsilon^x = \tilde{g}'(\cos\theta_- + \tau' \cos\theta_+)$ and $C_\epsilon^p = \tilde{g}'(\cos\theta_- - \tau' \cos\theta_+)$.

To determine the effective Hamiltonian explicitly, we need to combine it with the solution of the condition $C_{\sigma_x} = C_{\sigma_y} = C_{x\sigma_y} = C_{p\sigma_x} = C_x = C_y = 0$. There are two possible combinations of the transformations.

First, we set the transformation coefficients as $\theta_1 = \theta_2 = 0, p_0 = 0$, and

$$\begin{aligned}
\theta_3 &= \arccos \frac{4\gamma^2}{\tilde{g}^2(1 + \tau)^2} \\
x_0 &= \sqrt{\frac{\eta}{8\gamma^3}} \tilde{g}(1 + \tau) \sin\theta_3 \tag{15}
\end{aligned}$$

In this scenario, following the displacement transformation $x \rightarrow x + x_0$, the bound oscillator-form effective Hamiltonian implies a ground state with $\langle x^2 \rangle \propto x_0^2 \propto \eta$ and $\langle p^2 \rangle \propto \eta^0$. This characterizes the x-type SRP nature of the superradiant ground state. Furthermore, the energy gap can be expressed as

$$\begin{aligned}
\epsilon_{\text{xSRP}} &= \frac{2\gamma\omega}{(1 + \tau)^3 \tilde{g}_c^x \tilde{g}^2} \\
&\times \sqrt{[\tilde{g}^2(1 + \tau)^2 + 4\gamma^2] (\tilde{g}^2 - \tilde{g}_c^x) [4\tau - (1 - \tau)^2 \kappa \tilde{g}^2]}. \tag{16}
\end{aligned}$$

Second, we can also set the transformation coefficients as $\theta_1 = \theta_2 = \pi/2, x_0 = 0$, and

$$\begin{aligned}
\theta_3 &= \arccos \frac{4}{\tilde{g}^2(1 - \tau)^2} \\
p_0 &= -\sqrt{\frac{\eta}{8\gamma}} \tilde{g}(1 - \tau) \sin\theta_3. \tag{17}
\end{aligned}$$

In the scenario, considering the displacement transformation $p \rightarrow p + p_0$ performed, the bound oscillator-form effective Hamiltonian implies a ground state with $\langle x^2 \rangle \propto \eta^0$ and $\langle p^2 \rangle \propto p_0^2 \propto \eta$. This characterizes the p-type SRP nature of the superradiant ground state and yields the energy gap as

$$\begin{aligned}
\epsilon_{\text{pSRP}} &= \frac{2\omega}{(1 - \tau)^3 \tilde{g}_c^p \tilde{g}^2} \\
&\times \sqrt{[\tilde{g}^2(1 - \tau)^2 + 4] (\tilde{g}^2 - \tilde{g}_c^p) [(1 - \tau)^2 \kappa \tilde{g}^2 - 4\tau]}. \tag{18}
\end{aligned}$$

Next, we analyze the critical behavior of the energy gap. Along with the oscillator nature of the normal-phase system, as revealed by the effective Hamiltonian (7), the energy gap ϵ in the normal phase is given by

$$\epsilon = \frac{\omega}{4} \sqrt{\{4 - [(1 + \tau)^2 - 4\kappa] \tilde{g}^2\} [4 - (1 - \tau)^2 \tilde{g}^2]} \quad (19)$$

Next, we examine the critical behavior of the energy gap. Based on the oscillator nature of the normal-phase system, as described by the effective Hamiltonian (7), the energy gap

When approaching the triple point at $\tau = \kappa$, \tilde{g}_c^x and \tilde{g}_c^p should coalesce to \tilde{g}_c^{tri} . In this case, both the first and second radical factors of the normal-phase energy gap in Eq. (19) tends to vanish, leading to a distinct critical

behavior. Specifically, when approaching \tilde{g}_c^{tri} with fixed and identical τ and κ from the normal phase, the energy gap reduces to $\epsilon = \omega(1 - \tilde{g}^2/\tilde{g}_c^{tri2})$ and vanishes as $\epsilon \propto (\tilde{g}_c^{tri} - \tilde{g})$. Similarly, when approaching \tilde{g}_c^{tri} in the same way, but from the SRP, Eq. (18) predicts the vanishing of the energy gap as

$$\epsilon_{\text{pSRP}} \propto \sqrt{(\tilde{g} - \tilde{g}_c^p) \left[\tilde{g} - 2\sqrt{\tau/\kappa}/|1 - \tau| \right]} = \tilde{g} - \tilde{g}_c^{tri}.$$

Thus, this analysis supports a distinct energy-gap critical exponent $\beta_\epsilon = 1$ at the triple point, compared to $\beta_\epsilon = 1/2$ for the original SRPT, which is consistent with the numerical finite-size-scaling analysis in the main text.

-
- [1] R. H. Dicke, Phys. Rev. **93**, 99 (1954).
[2] K. Hepp and E. H. Lieb, Ann. Phys. **76**, 360 (1973).
[3] Y. K. Wang, F. T. Hioe, Phys. Rev. A **7**, 831 (1973).
[4] C. Emary and T. Brandes, Phys. Rev. Lett. **90**, 044101 (2003); Phys. Rev. E **67**, 066203 (2003).
[5] T. Niemczyk, F. Deppe, H. Huebl, E. P. Menzel, F. Hocke, M. J. Schwarz, J. J. Garcia-Ripoll, D. Zueco, T. Hümmer, E. Solano, A. Marx and R. Gross, Nat. Phys. **6**, 772 (2010).
[6] P. Forn-Díaz, J. Lisenfeld, D. Marcos, J. J. Garcia-Ripoll, E. Solano, C. J. P. M. Harmans, and J. E. Mooij, Phys. Rev. Lett. **105**, 237001 (2010).
[7] F. Yoshihara, T. Fuse, S. Ashhab, K. Kakuyanagi, S. Saito, and K. Semba, Nat. Phys. **13**, 44 (2016).
[8] J. S. Pedernales, I. Lizuain, S. Felicetti, G. Romero, L. Lamata, and E. Solano, Sci. Rep. **5**, 15472 (2015).
[9] M. L. Cai, Z. D. Liu, W. D. Zhao, Y. K. Wu, Q. X. Mei, Y. Jiang, L. He, X. Zhang, Z. C. Zhou, and L. M. Duan, Nat. Comm. **12**, 1126 (2021).
[10] S. Felicetti, E. Rico, C. Sabin, T. Ockenfels, J. Koch, M. Leder, C. Grossert, M. Weitz, and E. Solano, Phys. Rev. A **95**, 013827 (2017).
[11] A. Baksic and C. Ciuti, Phys. Rev. Lett. **112**, 173601 (2014).
[12] P. Kirton, M. M. Roses, J. Keeling and E. G. Dalla Torre, Adv. Quantum Technol. **2**, 1800043 (2018).
[13] M. J. Hwang, R. Puebla, and M. B. Plenio, Phys. Rev. Lett. **115**, 180404 (2015).
[14] I. I. Rabi, Phys. Rev. **51**, 652 (1937).
[15] M. J. Hwang and M. B. Plenio, Phys. Rev. Lett. **117**, 123602 (2016).
[16] M. X. Liu, S. Chesi, Z. J. Ying, X. Chen, H. G. Luo, and H. Q. Lin, Phys. Rev. Lett. **119**, 220601 (2017).
[17] L. T. Shen, Z. B. Yang, H. Z. Wu, and S. B. Zheng, Phys. Rev. A **95**, 013819 (2017).
[18] Y. Y. Zhang, Z. X. Hu, L. Fu, H. G. Luo, H. Pu, and X. F. Zhang, Phys. Rev. Lett. **127**, 063602 (2021).
[19] K. Rzażewski, K. Wódkiewicz, W. Żakowicz, Phys. Rev. Lett. **35**, 432 (1975).
[20] J. Keeling, J. Phys. Condens. Matter **19**, 295213 (2007).
[21] A. Vukics, T. Grießer, and P. Domokos, Phys. Rev. Lett. **112**, 073601 (2014).
[22] P. Nataf and C. Ciuti, Nat. Comm. **1**, 72 (2010).
[23] O. Viehmann, J. von Delft, F. Marquardt, Phys. Rev. Lett. **107**, 113602 (2011).
[24] C. Ciuti and P. Nataf, Phys. Rev. Lett. **109**, 179301 (2012).
[25] O. Viehmann, J. von Delft, F. Marquardt, arXiv, 1202, 2916.
[26] T. Jaako, Z. L. Xiang, J. J. Garcia-Ripoll, and P. Rabl, Phys. Rev. A **94**, 033850 (2016).
[27] G. M. Andolina, F. M. D. Pellegrino, V. Giovannetti, A. H. MacDonald, and M. Polini, Phys. Rev. B **100**, 121109(R) (2019).
[28] M. Bamba, K. Inomata, and Y. Nakamura, Phys. Rev. Lett. **117**, 173601 (2016).
[29] O. Di Stefano, A. Settineri, V. Macrì, L. Garziano, R. Stassi, S. Savasta, and F. Nori, Nat. Phys. **15**, 803 (2019).
[30] A. Stokes and A. Nazir, Phys. Rev. Lett. **125**, 143603 (2020).
[31] A. Stokes and A. Nazir, Rev. Mod. Phys. **94**, 045003 (2022).
[32] M. Bamba and N. Imoto, Phys. Rev. A **96**, 053857 (2017).
[33] O. Di Stefano, A. Settineri, V. Macrì, L. Garziano, R. Stassi, S. Savasta, and F. Nori, Nat. Phys. **15**, 803(2019).
[34] A. Stokes and A. Nazir, Phys. Rev. Lett. **125**, 143603 (2020).
[35] G. M. Andolina, F. M. D. Pellegrino, A. Mercurio, O. Di Stefano, M. Polini, and S. Savasta, arXiv:2104.09468v4.
[36] A. Baksic, P. Nataf, and C. Ciuti, Phys. Rev. A **80**, 023813 (2013).
[37] T. Liu, Y. Y. Zhang, Q. H. Chen, and K. L. Wang, Phys. Rev. Lett. A, **376**, 1962 (2012).
[38] Y. M. Wang, M. X. Liu, W. L. You, S. Chesi, H. G. Luo, and H. Q. Lin, Phys. Rev. A, **101**, 063843 (2020).
[39] X. Chen, Z. Wu, M. Jiang, X. Y. Lü, X. Peng, J. Du, Nat. Commun. **12**, 6281 (2021).
[40] X.-Y. Chen, L. W. Duan, D. Braak, and Q.-H. Chen, Phys. Rev. A **103**, 043708 (2021).
[41] Q. T. Xie, S. Cui, J. P. Cao, L. Amico, and H. Fan, Phys. Rev. X **4**, 021046 (2014).
[42] W. J. Yang and X. B. Wang, Phys. Rev. A **95**, 043823 (2017).
[43] S. I. Erlingsson, J. C. Egues, and D. Loss, Phys. Rev. B **82**, 155456 (2010).

- [44] I. C. Skogvoll, J. Lidal, J. Danon, and A. Kamra, Phys. Rev. Appl. **16**, 064008 (2021).
- [45] L. J. Zou, D. Marcos, S. Diehl, S. Putz, J. Schmiedmayer, J. Majer, P. Rabl, Phys. Rev. Lett., **113**, 023603 (2014).
- [46] X.-Y. Chen, Y.-Y. Zhang, Q.-H. Chen, H.-Q. Lin, arXiv:2405.19776 (2024).
- [47] J. Vidal and S. Dusuel, Europhys. Lett. **74**, 817 (2006).
- [48] Y. Wang, W. L. You, M. Liu, Y. L. Dong, H. G. Luo, G. Romero, and J. Q. You, New J. Phys. **20**, 053061 (2018).

